Journal of Inflammation Research

Dovepress
Taylor & Francis Group

Open Access Full Text Article

ORIGINAL RESEARCH

Transcriptomics and Network Pharmacology Reveal Anti-Inflammatory and Anti-Oxidative Stress Mechanisms of Qingxuan Runmu Yin in Dry Eye Disease

Shanshan Zhao[1,*], Jiadi Wang[1,2,*], Ying Liu[1], Xi Hu[1], Chenhao Gu[1], Jing Yao[1,2]

[1]Graduate School, Heilongjiang University of Chinese Medicine, Harbin, 150000, People's Republic of China; [2]Ophthalmology Department, The First Affiliated Hospital of Heilongjiang University of Chinese Medicine, Harbin, 150000, People's Republic of China

*These authors contributed equally to this work

Correspondence: Jing Yao, Ophthalmology Department, The First Affiliated Hospital of Heilongjiang University of Chinese Medicine, 26 Heping Road, Xiangfang District, Harbin, Heilongjiang, 150000, People's Republic of China, Tel +451-82111401, Email YJ00113@outlook.com

Purpose: Dry eye disease (DED) is a multifactorial chronic disorder of the ocular surface, characterized by reduced tear secretion, tear film instability, and inflammation. Oxidative stress is pivotal in DED pathogenesis. Qingxuan Runmu Yin (QRY) has shown substantial clinical efficacy in managing DED. This study aims to elucidate the molecular mechanisms underlying the antioxidant and anti-inflammatory effects of QRY in DED.

Methods: A benzalkonium chloride (BAC)-induced DED mouse model was established to evaluate QRY's protective effects on the ocular surface. RNA sequencing identified differentially expressed genes (DEGs, fold change >1.5, $P < 0.05$) among control, untreated DED, and QRY-treated DED mice. Transcriptomic analysis of DEGs was conducted. The active ingredients and targets of the ten Chinese herbal medicines in QRY were obtained from the TCMSP and TCMIP databases, whereas DED and oxidative stress-related genes were identified from the DisGeNET, OMIM, and GeneCards databases. A Chinese herbal medicine-active ingredient-target-disease network was constructed. The key pathways and targets of QRY against DED were investigated through transcriptomics and network pharmacology, and experimental validation was performed.

Results: QRY alleviated ocular surface damage in DED mice by repairing goblet cells, improving corneal damage, enhancing tear secretion, and reducing inflammatory factors and reactive oxygen species (ROS). Combined transcriptomic and network pharmacology analyses indicated that QRY reduced oxidative stress in DED by inhibiting pathways such as NF-κB and TNF. In vitro, QRY improved the survival of human corneal epithelial (HCE) cells damaged by oxidative stress. It inhibited the NF-κB signaling pathway and reduced levels of the pro-inflammatory cytokines IL-1β, IL-6, and TNF-α. In addition, QRY lowered ROS levels and enhanced superoxide dismutase (SOD) activity.

Conclusion: This study is the first to demonstrate that QRY mitigates ocular surface inflammation and oxidative stress in DED, providing a scientific foundation for its clinical application.

Keywords: dry eye disease, oxidative stress, inflammation, transcriptomics, network pharmacology, qingxuan runmu yin (QRY)

Introduction

Dry eye disease (DED) is a multifactorial chronic disease of the ocular surface, characterized by a decrease in tear secretion, tear film instability, and eye surface inflammation.[1,2] The disease often manifests as visual dysfunction and ocular discomfort, such as dryness, pain, and foreign body sensation, and has a prevalence ranging from 5% to 50%.[3,4] The disease may have a profound impact on a patient's quality of life and productivity, and is associated with mood disorders such as depression.[5]

https://doi.org/10.2147/JIR.S516780
Received: 30 January 2025
Accepted: 26 June 2025
Published: 8 January 2026

Graphical Abstract

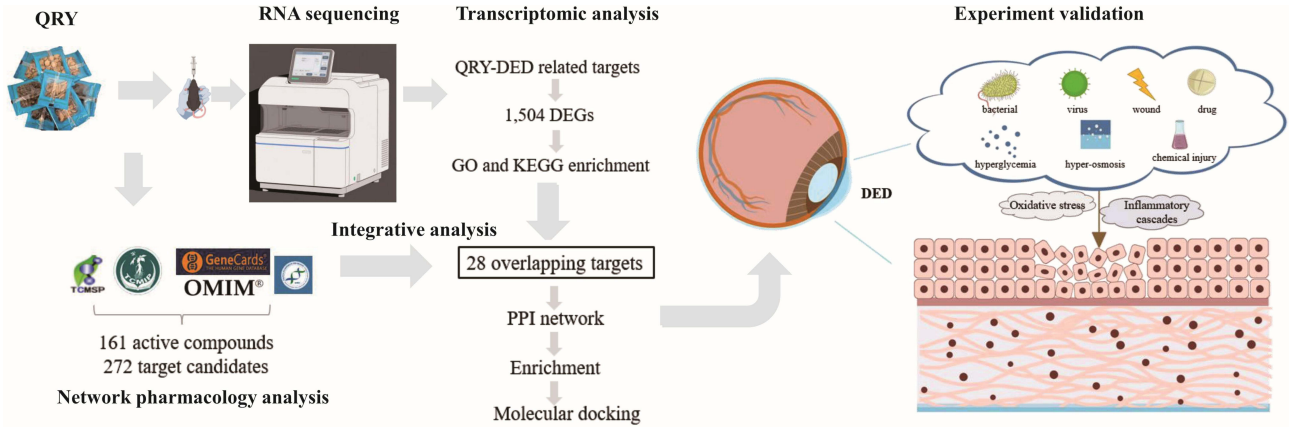

Although the causes of DED are complex, there is growing evidence that excessive accumulation of reactive oxygen species (ROS) and induction of oxidative stress play key roles in its development.[6–8] Excess ROS directly damages intracellular DNA, proteins, lipids, and other crucial substances, resulting in damage to the cornea, conjunctiva, and lacrimal glands. This leads to tear film hyperosmolarity and decreased tear film stability, which triggers the development of DED.[9,10] In addition, excessive oxidative stress results in high levels of intracellular ROS that act as upstream mediators to activate the NF-κB and MAPK signaling pathways, thereby stimulating the expression of a variety of inflammatory factors.[11] This, in turn, leads to the core mechanism of DED, the development of inflammation on the ocular surface. These inflammatory factors can also lead to corneal epithelial damage and tear film instability, exacerbating dry eye symptoms and creating a vicious cycle.[12] Taken together, these findings show that oxidative stress injury plays a crucial role in the development and prognosis of DED. To date, the treatment of DED remains a considerable challenge in ophthalmology, with the majority of commonly used therapeutic agents having limitations, such as localized symptomatic relief, short duration of efficacy, susceptibility to adverse effects, and increased risk of cataracts and opportunistic infections.[13,14]

Traditional Chinese Medicine (TCM), with a documented history spanning over two millennia, has recently gained scientific interest for its potential role in managing chronic diseases of multifactorial etiology. Accumulating evidence from clinical trials and systematic reviews supports the therapeutic utility of certain TCM formulations. For instance, *Lycium barbarum* (Goji berry) has provided a neuroprotective effect for the retina in retinitis pigmentosa, while *Tripterygium wilfordii* (Thunder God Vine) has demonstrated efficacy in alleviating rheumatoid arthritis symptoms by suppressing pro-inflammatory cytokines.[15,16] Nevertheless, comprehensive mechanistic studies remain imperative to validate their multi-target actions and refine therapeutic regimens. Qingxuan Runmu Yin (QRY) is a representative TCM formula developed by Professor Yao Jing, a renowned Chinese medicine expert, through modification of the Zengye decoction (ZYD) for DED treatment. Previous studies have demonstrated that QRY exhibits significant clinical efficacy.[17] Our research has shown that QRY improves tear secretion, repairs corneal damage, and affects ferroptosis in DED rats.[18] Furthermore, numerous studies have indicated that ZYD, the foundational prescription of QRY, has pharmacological properties such as antioxidant and anti-inflammatory effects, which help alleviate clinical symptoms of Sjögren's syndrome (SS).[19] Additionally, the components of QRY, including various traditional herbs, have demonstrated therapeutic effects in treating DED. For instance, extracts from *Dendrobium officinale* alleviate dry eye inflammation by modulating aquaporins and targeting the MAPK/NF-κB signaling pathway.[20] Chrysoeriol from *Lonicerae Japonicae Flos* has been shown to enhance retinal function through its antioxidant properties and suppress inflammation via inhibition of NF-κB signaling.[21,22] Liquiritigenin and liquiritin, isolated in *licorice*, and Ophiopogonin D, extracted from *Radix Ophiopogon japonicus*, have been shown to exhibit strong anti-inflammatory and antioxidant effects.[23,24] Moreover, Quercetin, a compound found in several QRY

herbs, including *Forsythiae Fructus, Lonicerae Japonicae Flos*, and *licorice*, has also shown promising therapeutic potential in DED treatment.[25] However, unlike monomeric compounds, QRY, as a TCM formula, consists of multiple components and targets, so its specific mechanism in the treatment of DED remains obscure.

High-throughput RNA sequencing (RNA-Seq) is a crucial technological approach for conducting transcriptomics research, and is therefore useful for identifying differentially expressed genes and unraveling specific biological processes involved in disease development.[26] Network pharmacology is an emerging field based on disease phenotypes, genes, and drugs, and recently has been used extensively for target gene prediction and multi-target interactions.[27] The complexity of chemical components and molecular mechanisms in Chinese herbal formulas is compatible with the multi-target and multi-pathway nature of network pharmacology. Therefore, we used the combined strategy of transcriptomics and network pharmacology to identify the active ingredients, targets, and potential mechanisms of action of QRY in DED. In addition, in vitro experiments were conducted to verify the pharmacological antioxidant effects of QRY.

Materials and Methods

Animal Experimentation

Herbs and Reagents

Ten grams of each of the following herbs were sourced from the First Hospital Affiliated to Heilongjiang University of Traditional Chinese Medicine. QRY: *Atractylodes Macrocephala Koidz*. (Bai Zhu), *Ophiopogon japonicus (L.f) Ker-Gawl*. (Mai Dong), *Figwort Root* (Xuan Shen), *Rehmannia glutinosa Libosch* (Di Huang), *Forsythiae Fructus* (Lian Qiao), *Lonicerae Japonicae Flos (Jin Yinhua), Dendrobium nobile Lindl* (Shi Hu), *Saposhnikoviae Radix* (Fang Feng), *Platycodon Grandiforus* (Jie Geng) *and Licorice* (Gan Cao). Benzalkonium chloride (BAC) was obtained from the Aladdin Biochemical Technology Co. (Shanghai, China). Phenol red cotton threads were obtained from Jingming New Technology Development Co. Ltd. (Tianjin, China). Periodic acid-Schiff (PAS) kits and Phosphate Buffered Saline (PBS) were acquired from Solarbio (Beijing, China). Eyeball fixed liquid was obtained from Powerful Biology Co. (Wuhan, China). The IL-1β and IL-6 ELISA kits were obtained from Shanghai Enzyme-linked Biotechnology Co., Ltd. (Shanghai, China). The ROS ELISA kit was acquired from COIBO Biotechnology Co. Ltd. (Shanghai, China).

Animals

Female C57BL/6J mice (6–8 weeks old, SPF grade, weighing 16–18 g) were provided by Liaoning Changsheng Biotechnology Co. Ltd. (SCXK [Liao] 2020–0001), and maintained in the Laboratory Animal Center of Heilongjiang University of Traditional Chinese Medicine. The mice had free access to food and water, and were housed at a temperature of 25 ± 2°C, relative humidity of 50 ±10%, and a 12 h/12 h alternating light and dark cycle. This study followed the ethical guidelines for animal welfare. All experimental procedures were approved by the Ethics Committee of Heilongjiang University of Traditional Chinese Medicine (HLJUTCM2023090601) and strictly complied with China's national standard GB/T 35892–2018 "Guidelines for Ethical Review of Laboratory Animal Welfare".

Grouping and Processing

Mice were randomly assigned to three groups (n = 20 per group): normal, model, and QRY groups. Except for the normal group, mice in the other two groups were administered 5 μL of 0.2% BAC solution into the conjunctival sac of both eyes twice daily for 14 days to create a model of DED. After the model was developed, the dose of drug administered to the mice was converted to the equivalent surface area of a human, with mice in the QRY group administered 18.50 g/kg of QRY by gavage twice a day for 14 days. Mice in the normal and model groups received the same volume of distilled water via gavage. The experiment lasted for 28 days.

Phenol Red Thread (PRT) Test

Phenol red cotton thread was placed in the lower conjunctival sac of each mouse for 1 min. The length of the wetted portion was measured using calipers. Mean values were derived from measurements collected from both eyes. Tear secretion was measured on days 1, 14, and 28 throughout the experiment.

Corneal Fluorescein Staining (FL)

A 20 μL aliquot of 1% fluorescein sodium was dropped into the mouse conjunctiva for 1 min. This was followed by corneal epithelial staining observed under a cobalt blue filter using a slit-lamp microscope and photography for scoring. The cornea was divided into four quadrants and scored separately, with each quadrant accumulating a score of 0–4, as follows: 0, no staining; 1, ≤30 punctate staining; 2, >30 punctate staining; 3, diffuse staining without stained plaques; and 4, stained plaques. The final score was calculated as the sum of the scores in the four quadrants.[28,29]

Histological Analysis

Following deep anesthesia, all mice were humanely euthanized. Eyeballs were immediately enucleated and placed into centrifuge tubes containing eyeball-fixed liquid, then maintained at room temperature for 24 hours. Standard hematoxylin and eosin (HE) staining was performed, including dehydration, embedding, and staining, to observe pathological changes in the corneal tissue using a microscope (BX53; Olympus, Tokyo, Japan).

Goblet Cell Detection

Paraffin-embedded sections of the conjunctiva were stained with PAS. Microscopic observations were performed at 200× magnification and the number of goblet cells in three randomly selected fields was averaged.

ELISA Assay

Corneal tissues were homogenized in pre-cooled PBS (tissue mass-to-PBS volume ratio of 1:9) and centrifuged to collect supernatants. ELISA plates were loaded with 100 μL of either the tissue supernatant or the standard solution and processed according to the manufacturer's instructions. OD values were measured at a wavelength of 450 nm using a microplate reader (SpectraMax® i3x, Molecular Devices, CA, USA).

RNA-Seq Assay

The Illumina NovaSeq 6000-based sequencing platform was used for high-throughput sequencing. We extracted RNA samples from three groups of mouse corneas (n=3), which were examined and qualified for reverse transcription, amplification, and on-board sequencing.[30] The rRNA sequences were then removed using SortMeRNA.[31] Clean reads were obtained by Trimmomatic filtration and compared to the reference genome using Hisat2, with the genome comparison of each sample counted.[32] The RNA-seq was performed by Ouyi Bio Comp. (Shanghai).

Transcriptomic Analysis

Genes were filtered using counts with a mean value > 2. DESeq2 software was used to calculate the differential fold changes of the genes in each sample, with the thresholds for differentially expressed genes (DEGs) set as fold change (FC) >1.5 and $P < 0.05$. Volcano and heat maps were plotted using the ggplot2 package in R language.

Network Pharmacology Construction and Bioinformatics Analysis

Active Compounds and Targets

The active compounds of the ten QRY herbs were obtained from the Traditional Chinese Medicine Systems Pharmacology Database (TCMSP) (https://old.tcmsp-e.com/tcmsp.php) and an Integrative Pharmacology-based Research Platform of Traditional Chinese Medicine (TCMIP) (http://www.tcmip.cn/ETCM/). Oral bioavailability (OB) ≥ 30%, drug-likeness (DL) ≥ 0.18 (or drug-likeness weight ≥0.49) were used to screen for active compounds. Gene names corresponding to drug targets were obtained from the UniProt protein database (https://www.uniprot.org/).

DED and Oxidative Stress-Related Candidate Targets

Disease-related genes were searched using the keywords "dry eye" and "oxidative stress" in Genecards (https://www.genecards.org/), DisGeNET (https://www.disgenet.org/), and OMIM (http://www.omim.org/) databases. Using the above targets, candidate targets were obtained from the overlap of the active compound-related targets.

Network Construction and Functional Enrichment Analysis

A composite network was constructed using the Cytoscape 3.9.1 software (https://cytoscape.org/) to link herbs, active compounds, and candidate targets. In the network, molecular species such as active ingredients and proteins are represented as nodes, whereas the interactions between these molecular species are represented as edges.

Gene Ontology (GO) and Kyoto Encyclopedia of Genes and Genomes (KEGG) Analyses

GO and KEGG analyses were conducted using the Database for Annotation, Visualization, and Integrated Discovery (DAVID, https://david.ncifcrf.gov/), with a screening result threshold of $P<0.05$.

Protein-Protein Interaction (PPI) Analysis and Nucleus Target Genes

The candidate target genes were overlapped with DEGs using Venny 2.0 and identified as key target genes, while the PPI network was constructed using the String database. We calculated the degree (D), betweenness centrality (BC), and closeness centrality (CC) of the PPI network. Cytosolic target genes were selected from the top six genes with the maximum D values.

Molecular Docking

The molecular structure (Mol2 structure) of the main active compounds was obtained from PubChem (https://pubchem.ncbi.nlm.nih.gov/). The 3D structure of the core target protein was obtained from the Research Collaboratory for Structural Bioinformatics Protein Data Bank (RCSB PDB; https://www.rcsb.org/). After removing water, hydrogenation, charge calculation, and non-polar hydrogen using MGLTools v1.5.7 (https://ccsb.scripps.edu/mgltools/), docking was performed using AutoDock Vina v1.2.3 (http://vina.scripps.edu/). Using a threshold of −5.0 kcal/mol as the criterion for effective receptor-ligand interactions, select the highest scoring conformational isomer and visualize PyMOL Molecular Graphics System v2.5.2 (https://pymol.org/).

Experimental Validation

Cell Culture and Preparation of Drug-Containing Serum

Human corneal epithelial (HCE) cells were supplied by Procell Life Science & Technology Co., Ltd. and cultured in DMEM supplemented with 10% fetal bovine serum (FBS), 100 U/mL penicillin, and 100 mg/mL streptomycin in a humidified incubator at 37°C with 5% CO_2. The QRY was prepared as previously described. Sprague Dawley (SD) rats were randomly divided into control, low-dose, and high-dose groups, with five rats in each group. The dosage was calculated according to the equivalent body surface area of humans and rats (low-dose group,4.5 g/kg/d, high-dose group,9 g/kg/d), and the drug was administered by gavage for five consecutive days. Blood samples were collected one hour after the final administration and serum was obtained via centrifugation. After heat inactivation at 56°C for 30 min, the serum was filtered and stored at −80°C for subsequent experiments.

4-HNE Cytotoxicity Screening

The HCE cells were inoculated into 96-well plates, and each well was treated with different concentrations of 4-HNE (0, 10, 20, 30, and 40 μM). The toxicity of these concentrations on the cells was detected by CCK-8 after 12 h or 24 h of induction.

QRY Cytotoxicity Assay

HCE cells in logarithmic growth phase were collected and inoculated into 96-well plates. Control, model, QRY-L (4-HNE+ low-drug-containing serum), and QRY-H (4-HNE+ high-drug-containing serum) groups. Except for the control group, all other groups were administered 4-HNE to induce oxidative stress. The corresponding drug serum was then added to each treatment group. CCK8 reagent was added after 24 h of incubation in a constant-temperature incubator. The absorbance of each well was measured to determine cell viability.

ROS Activity Assays

ROS detection reagent (AAT Bioquest) was used as the working solution. The cells were incubated with the working solution for 1h in a constant-temperature box at 37 °C and 5% CO2, after which the test compound was added. Fluorescence intensity

after stimulation was detected using a fluorescence spectrophotometer with an excitation wavelength of 490 nm and an emission spectrum of 525 nm (PF-8500, Jasco, Tokyo, Japan).

Superoxide Dismutase (SOD) ELISA Assay

After the treatment of each group of HCE cells, the cells and cell culture supernatants were collected, and SOD activity was measured and plotted statistically according to the steps described in the kit (Shanghai Enzyme-linked Biotechnology Co).

TUNEL Assay for Apoptosis Detection

The assay was performed using the TUNEL Apoptosis Detection Kit, with the test procedure carried out according to the manufacturer's instructions (Beyotime Biotechnology). The early apoptosis rate was analyzed using fluorescence microscopy.

Western Blot Analysis

HCE cells were lysed using the radioimmunoprecipitation assay, and the total protein concentration was measured using the BCA method. The total protein concentration was adjusted to 2.0 μg /μL and a 10 μL aliquot was then electrophoresed on 10% SDS-polyacrylamide gels, followed by wet transfer of the products onto a PVDF membrane. The membrane was blocked with 5% skimmed milk powder at room temperature, followed by the addition of primary and secondary antibodies and further incubation and washing. The ECL mixture was then added uniformly in drops and images were captured using a fully automated chemiluminescence gel imaging system. Primary antibodies used were IL-1β, IL-6, TNF-α, and P65 (Proteintech). p-P65 (Abcam).

Statistical Analysis

GraphPad Prism 9.5 software was used for the statistical analysis of the data. The results of the measurement data were expressed as mean ± standard deviation ($x \pm s$), and comparisons between multiple groups analyzed by one-way ANOVA, with $P < 0.05$ indicating statistically significant differences.

Results

QRY Protects the Ocular Surface Barrier in BAC-Induced DED Mouse Model

Corneal epithelial damage was assessed using fluorescein staining, which selectively highlights areas of epithelial compromise. As illustrated in Figures 1A and B, mice exhibited pronounced corneal epithelial defects by day 14 post-induction, evidenced by extensive fluorescein uptake. Additional hallmark features of DED were observed following model establishment, including decreased tear production, disruption of corneal epithelial architecture, and a marked reduction in conjunctival goblet cell density (Figures 1C and E). Furthermore, elevated levels of pro-inflammatory cytokines (IL-1β and IL-6) and reactive oxygen species (ROS) in corneal tissues corroborated the successful induction of ocular surface inflammation characteristic of DED (Figure 1F).

By day 28, the QRY group showed notable improvements, including increased tear secretion, reduced FL scores, restored corneal epithelial structure, and enhanced goblet cell populations. Additionally, IL-1β, IL-6, and ROS levels were significantly reduced, indicating that QRY effectively alleviated corneal damage, increased tear production, and mitigated inflammation and oxidative stress in BAC-treated DED mice.

DEGs and Pathways Identified by RNA-Seq and Transcriptomic Analysis

RNA-Seq analysis revealed distinct gene expression profiles in the control, model, and QRY-treated groups (Figure 2A). A total of 3,717 DEGs were identified between the control and model groups, including 2,175 upregulated and 1,542 downregulated genes (Figure 2B) (The DEGs can be found as Supplementary Table S1). In the QRY-treated versus model group comparison, 1,504 DEGs were identified, with 746 upregulated and 758 downregulated genes (Figure 2C) (The DEGs can be found as Supplementary Table S2). Heatmap analysis confirmed the significant differences in expression between the QRY-treated and model groups (Figure 2D).

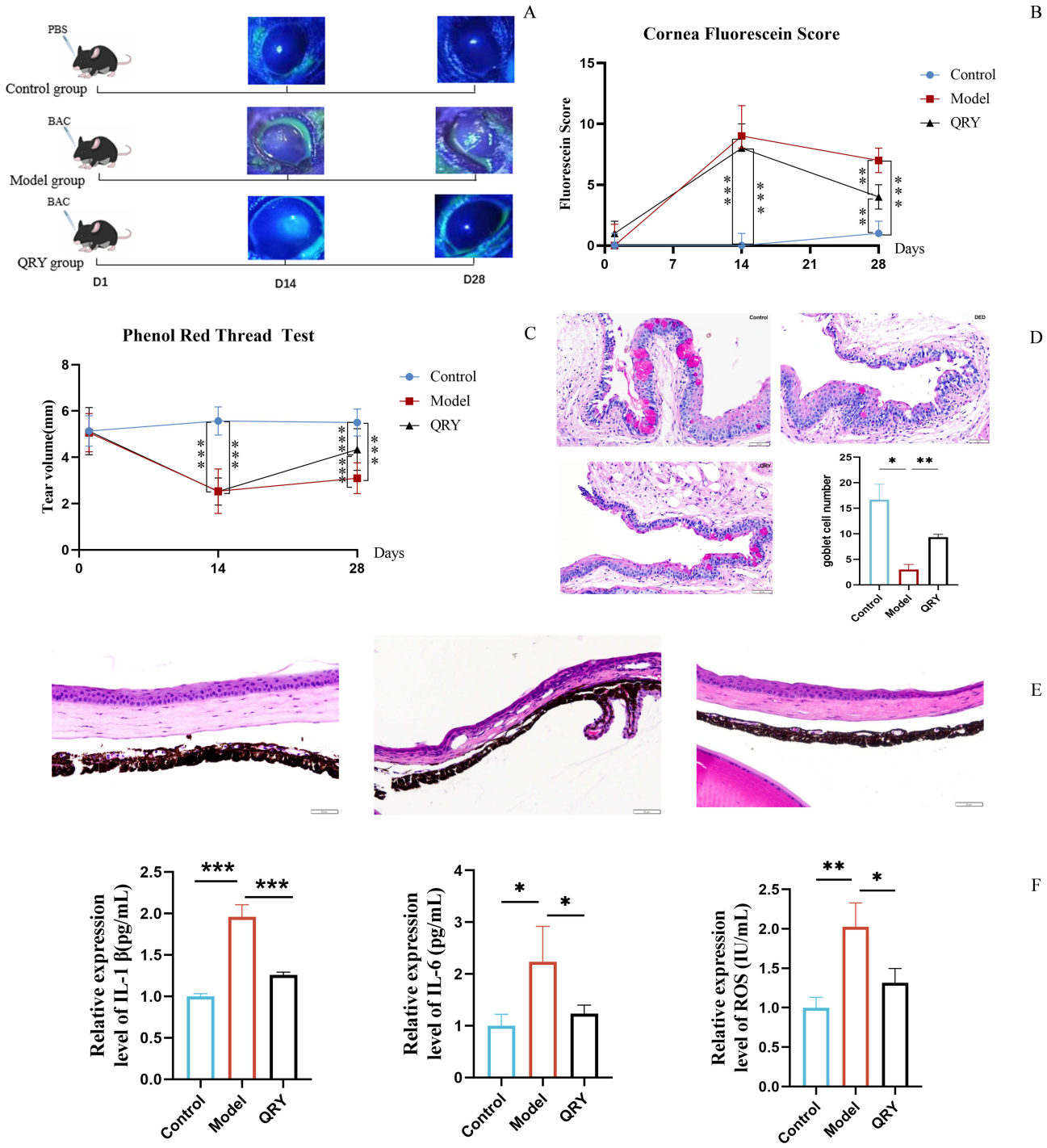

Figure 1 QRY treatment of mice with BAC-induced DED. (**A**) The staining status of fluorescein sodium and fluorescein in each group. (**B**) Evaluate FL score on days 1, 14, and 28 (n=20). (**C**) Measure tear secretion on days 1, 14, and 28, (n=20). (**D**) PAS staining results of conjunctival goblet cells in each group, (magnification×200, n=3). (**E**) HE staining results of corneal tissues in each group, (magnification×200). (**F**) ELISA detection of IL-1β, IL-6, and ROS levels in corneal tissues of each group. Data are presented as the $\bar{x} \pm s$. $P < 0.05$, $^{**}P < 0.01$ and $^{***}P < 0.001$vs. model group.

GO enrichment analysis revealed that DEGs were primarily associated with biological processes such as immune response, inflammatory response, extracellular matrix organization, and transmembrane transport (Figure 2E). KEGG pathway analysis indicated enrichment in inflammation and oxidative stress-related pathways, including the JAK-STAT, IL-17, TNF, and cytokine-cytokine receptor interaction pathways (Figure 2F).

https://doi.org/10.2147/JIR.S516780

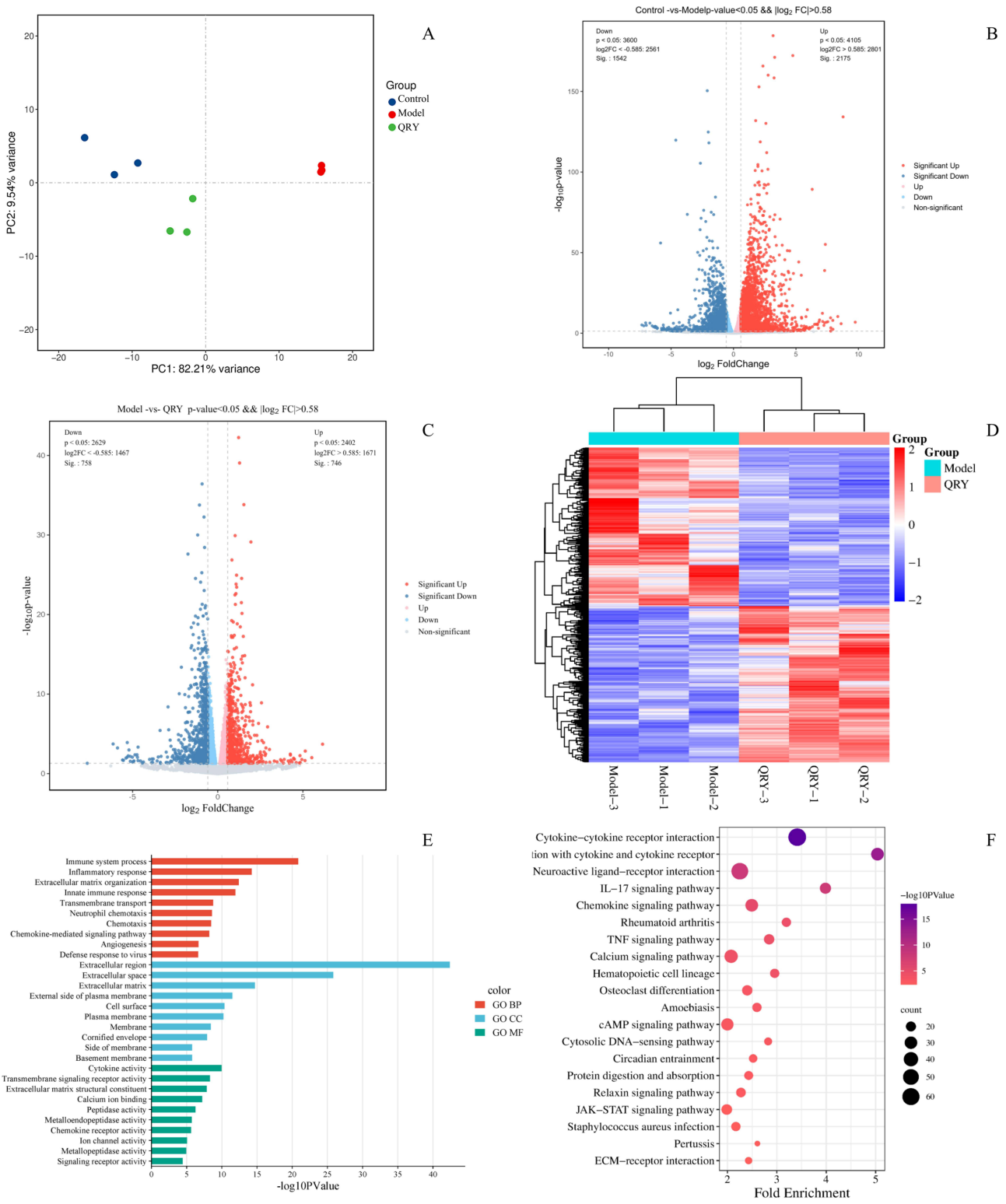

Figure 2 Analysis of differentially expressed genes (DEGs) in the mice with BAC-induced DED. (**A**) PCA mapping of Control, Model, and QRY samples. (B)Volcanic plot analysis of DEGs in the control group of mice vs the model group using a threshold of FC >1.5 and *P* <0.05. (**C**) Volcanic plot analysis of DEGs in the QRY group of mice vs the model group using a threshold of FC >1.5 and *P* <0.05. (**D**) Heatmaps created based on DEGs. Red and green represent up and down-regulation of gene expression, respectively. (**E**) GO analysis of DEGs in QRY-treated mice with DED. (**F**) KEGG pathway analysis of DEGs in QRY-treated mice with DED.

https://doi.org/10.2147/JIR.S516780

Network Pharmacology Analysis

To further investigate the mechanism of QRY in DED, we conducted network pharmacology analysis. A total of 161 active compounds, including 7 from *Atractylodes Macrocephala Koidz*., 18 from *Saposhnikoviae Radix*, 23 from *Forsythiae Fructus*, 88 from *licorice*, 23 from *Lonicerae Japonicae Flos*, 7 from *Platycodon Grandiforus*, and 9 from *Figwort Root*, were identified based on OB ≥ 30% and DL ≥ 0.18 in the TCMSP database. The TCMIP database was used to search for *Ophiopogon japonicus (L.f) Ker-Gawl., Dendrobium nobile Lindl*, and *Rehmannia glutinosa Libosch* not yet included in TCMSP, with 35 active compounds of *Ophiopogon japonicus (L.f) Ker-Gawl*., 24 of *Dendrobium nobile Lindl*, and 1 of *Rehmannia glutinosa Libosch* obtained using a drug likeness weight ≥0.49 as the screening condition. After removing duplicates, 220 active compounds were identified in QRY, among which kaempferol, adenosine, and quercetin were common to several herbs (The entire list of active compounds can be found as Supplementary Table S3). Subsequently, 462 compound-related targets were identified by screening the TCMIP and TCMSP databases (The entire list of targets can be found as Supplementary Table S4). Screening of three databases, GeneCards, OMIM, and DisGeNET, then yielded 4,581 DED-related targets and 12,280 oxidative stress-related targets (The entire list of targets can be found as Supplementary Table S5). The overlapping targets between the three target datasets described above were identified as candidate targets to assess the use of QRY in the treatment of DED based on their antioxidative stress action (Figure 3A).

To determine the overall function of QRY, we created a herb component–target network comprising 10 herbs, 161 active compounds, and 272 target candidates. Among these compounds, quercetin, adenosine, kaempferol, luteolin, and wogonin were the top five relevant candidate compounds, with 120, 59, 46, 46, and 33 candidate targets, respectively. (Figure 3B).

Functional enrichment analysis of 272 candidate targets was performed using DAVID software. GO analysis revealed these potential therapeutic targets were significantly enriched in the paths of "response to hypoxia", "negative regulation of apoptosis", etc. (Figure 3C).

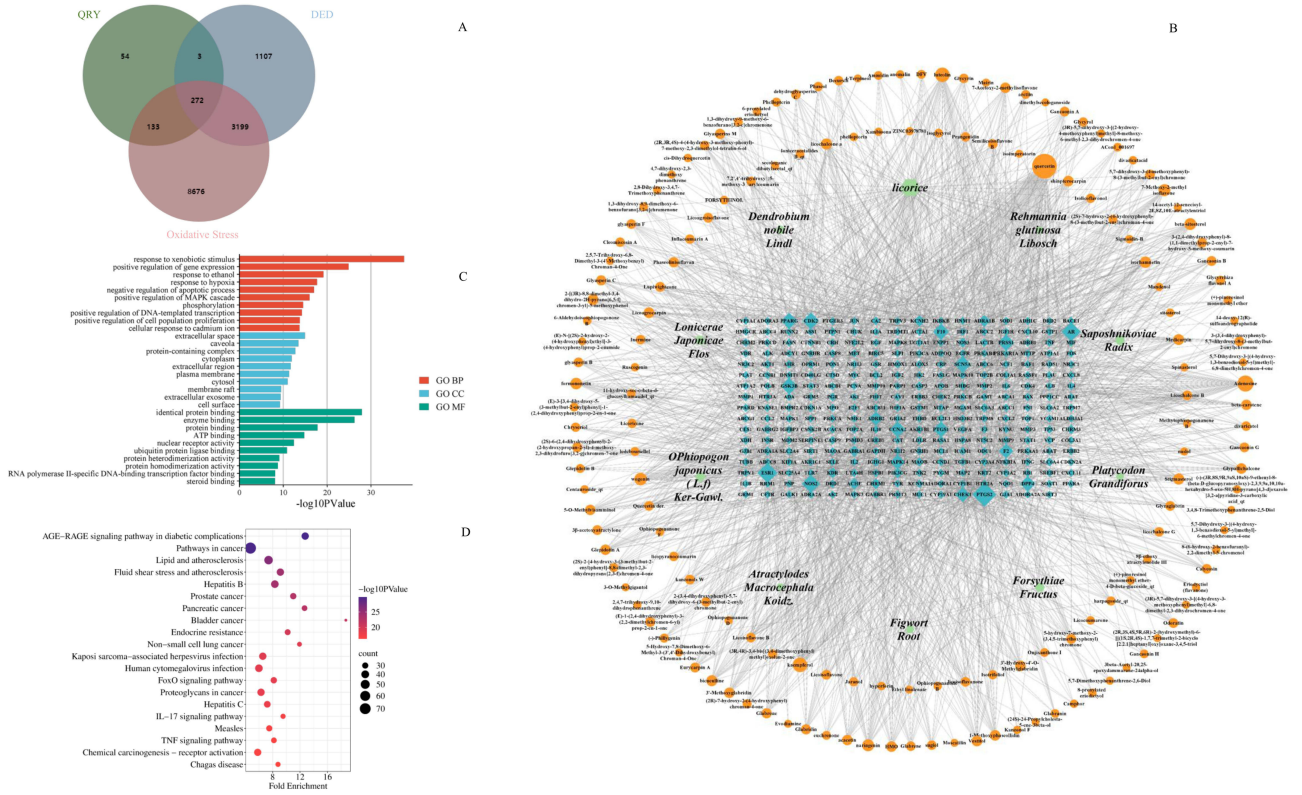

Figure 3 Network analysis of herb-active compounds-candidate targets, and GO and KEGG analyses. (**A**) Cross-Gene Venn diagrams related to dry eye disease, oxidative stress, and QRY. (**B**) Network analysis diagram of 10 herbal compositions, 220 active compounds, and 272 candidate targets of QRY. (**C**) Top 10 BP, CC, and MF terms based on a *P* value <0.05. (**D**) Top 20 pathways obtained based on a *P* <0.05 in the KEGG analysis.

https://doi.org/10.2147/JIR.S516780

KEGG analysis highlighted pathways involved in immune and inflammatory responses, such as the AGE-RAGE, TNF, and IL-17 signaling pathways (Figure 3D). Notably, the TNF and IL-17 pathways showed significant overlap with the transcriptomic results, suggesting their pivotal role in QRY-mediated DED therapy.

Combined Analysis of Transcriptomics and Network Pharmacology

To gain deeper insights into the mechanisms of QRY therapy for DED, integrated analysis of transcriptomic and network pharmacological data was performed. Twenty-eight overlapping key targets were identified by comparing DEGs from RNA-seq with candidate targets derived from network pharmacology (Figure 4A). PPI analysis of these targets revealed a network

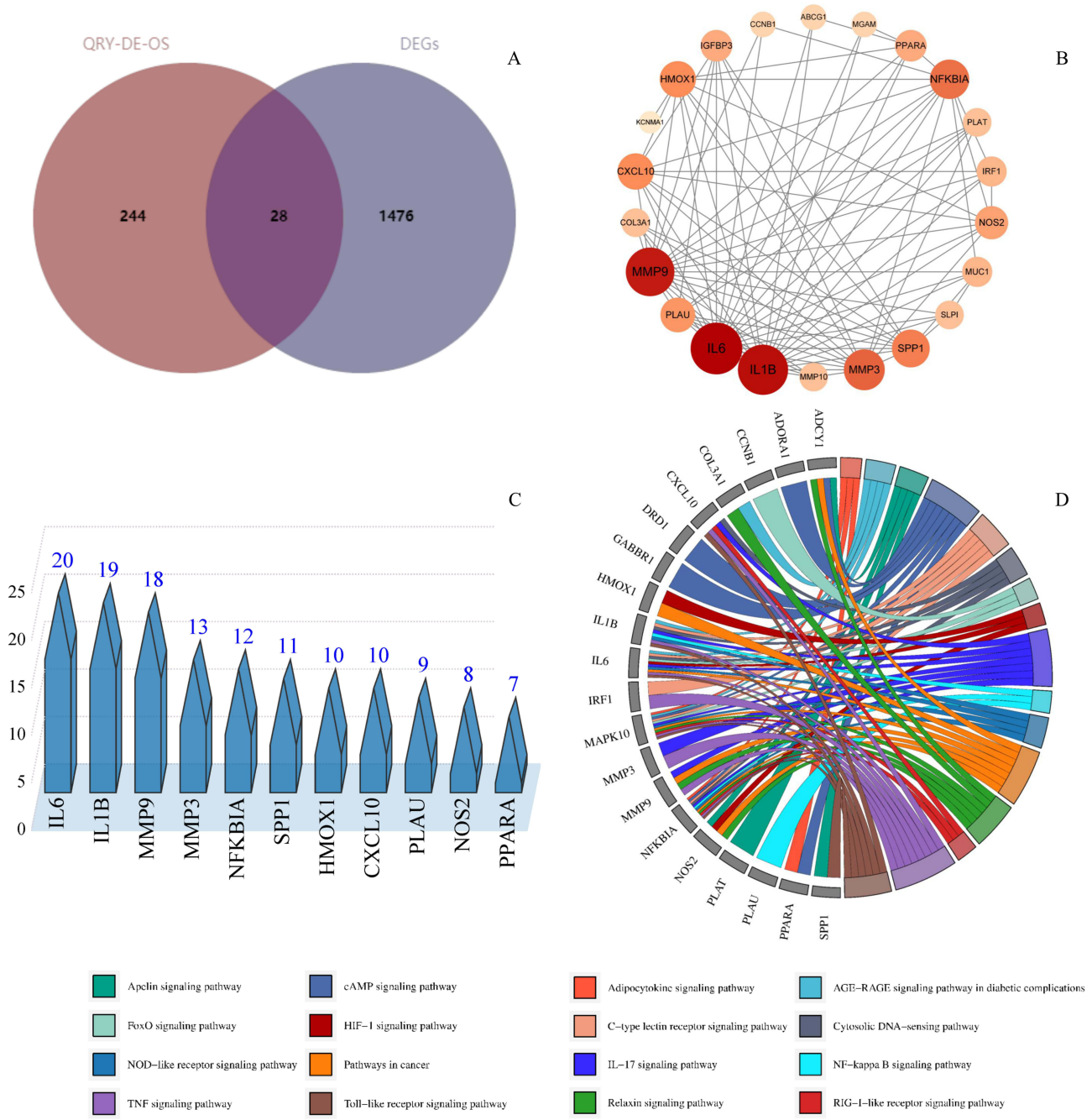

Figure 4 Screening and analysis of nucleus targets. (**A**) Venn diagram of network pharmacology combined with RNA-seq screening of QRY key targets. (**B**) PPI network analysis of 28 key targets. (**C**) Discovery of 11 core targets for QRY anti-oxidative stress treatment of DED according to D, BC, and CC. (**D**) The pathways analyzed by chordal plots.

https://doi.org/10.2147/JIR.S516780

comprising 22 nodes and 93 edges after excluding isolated targets (Figure 4B). Eleven core targets, including IL-1β, IL-6, MMP9, NFκBIA, and HMOX1, were identified based on median values of degree (D), betweenness centrality (BC), and closeness centrality (CC), highlighting QRY's potential roles in anti-inflammatory and anti-oxidative stress actions (Figure 4C). Functional pathway analysis of these core targets using KEGG identified key pathways, including IL-17, TNF, TLR, and NF-κB, which are critical to the therapeutic effects of QRY. Chord diagrams were used to clearly display gene enrichment between pathways, showing that the TNF and NF-κB signaling pathways were significantly enriched. Previous studies have demonstrated that these pathways play a critical role in inflammatory and oxidative stress responses.[33] Based on these results, we hypothesize that QRY exerts therapeutic effects on DED through anti-inflammatory and antioxidant mechanisms (Figure 4D).

Molecular Docking

The main compounds in QRY (quercetin, adenosine, luteolin) were docked with three core targets obtained from PPI (IL-1β, IL-6, MMP9). The results showed that the binding energies of quercetin, adenosine, and kaempferol with IL-1β, IL-6, and MMP9 ranged from −6.2 kcal/mol to −8.3 kcal/mol (Table 1). This suggests that the core targets exhibit enhanced affinity for the active compounds (Figure 5).

Screening of 4-HNE Concentrations for HCE Cell Models

As 4-hydroxynonenal (4-HNE) is an essential marker of lipid peroxidation and has been widely used to induce oxidative stress in cells.[34–36] Firstly, we investigated the effect of different concentrations of 4-HNE on HCE cell viability. As illustrated in Figure 6A, HCE cells treated with 10 μM 4-HNE for 24 hours displayed significantly higher viability compared to untreated control cells. This phenomenon may be attributed to the hormesis effect of low-concentration 4-HNE, which activates endogenous antioxidant pathways.[37] The viability of HCE cells treated with 20 μM, 30 μM, and 40 μM 4-HNE-treated HCE cells also decreased with time. Finally, we selected the 20 μM 4-HNE-induced HCE cell model for use in subsequent experiments.

QRY Cytotoxicity Assay

Next, we investigated the effects of different concentrations of QRY on the 4-HNE-induced HCE cell model. As shown in Figure 6B, compared to the model group, cell viability in the QRY-L and QRY-H groups increased significantly, with the greatest increase observed in the QRY-H group.

Table 1 Screening Docking Results Between Ligands and Receptors

Hub Targets (PDB ID)	Active Ingredients	Binding Energy (Kcal/Mol)
IL-1β (1HIB)	Quercetin	−7.1
	Adenosine	−6.3
	Kaempferol	−7.1
IL-6 (1ALU)	Quercetin	−7.1
	Adenosine	−6.2
	Kaempferol	−6.6
MMP9 (6ESM)	Quercetin	−8.3
	Adenosine	−7.9
	Kaempferol	−6.7

https://doi.org/10.2147/JIR.S516780

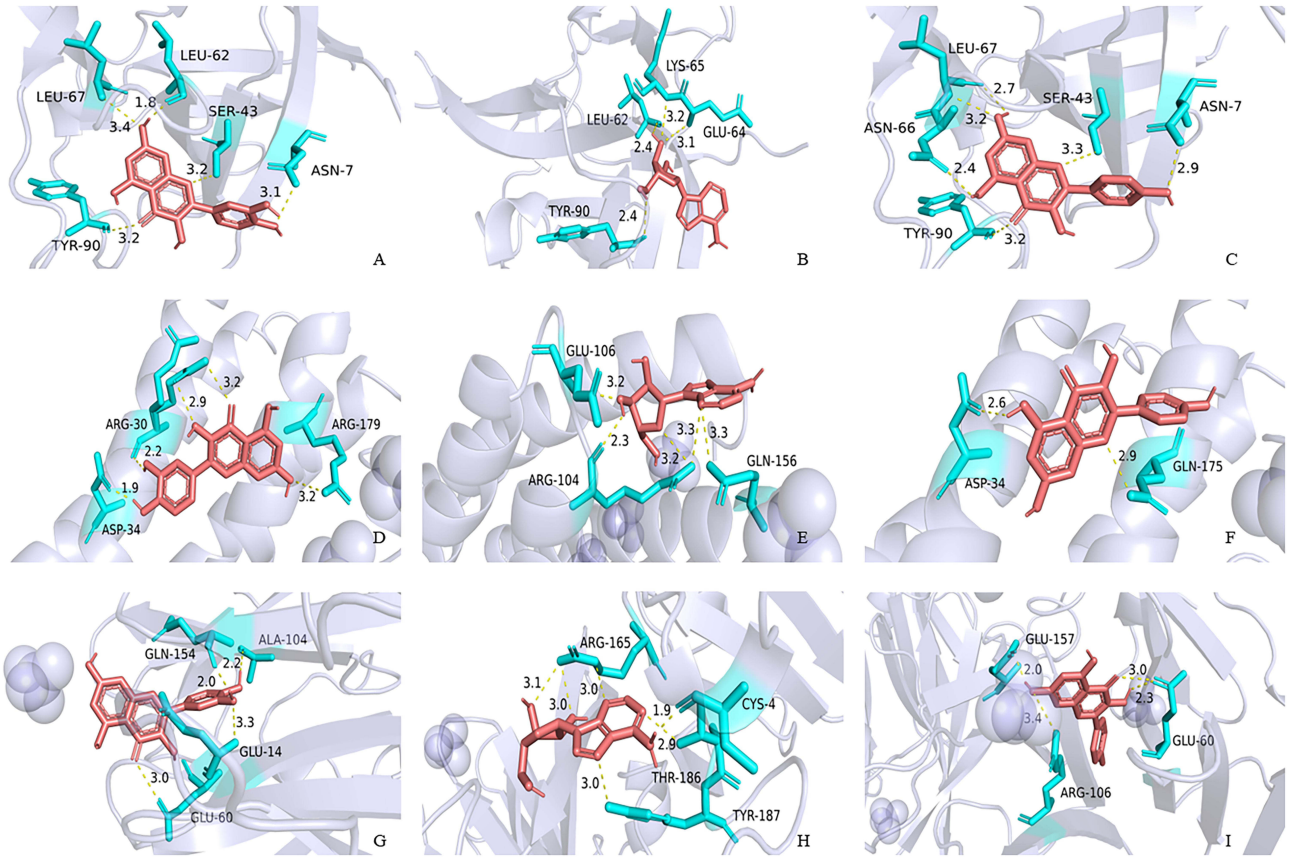

Figure 5 Quercetin, adenosine, kaempferol docking models with IL-1β, IL-6 and MMP9, respectively. (**A**) IL-1β action model with quercetin. (**B**) IL-1β action model with adenosine. (**C**) IL-1β action model with kaempferol. (**D**) IL-6 action model with quercetin. (**E**) IL-6 action model with adenosine. (**F**) IL-6 action model with kaempferol. (**G**) MMP9 action model with quercetin. (**H**) MMP9 action model with adenosine. (**I**) MMP9 action model with kaempferol.

Effect of QRY on Intracellular ROS Levels

The intracellular ROS levels were significantly higher in the model group than in the control group. The intracellular ROS levels were significantly lower in the QRY-H group than in the model group, although the difference was not significant (Figure 6C).

Effect of QRY on Intracellular SOD Activity

The intracellular SOD activity was significantly lower in the model group than in the control group. Intracellular SOD activity in the QRY-H group was significantly higher than that in the model group. Notably, intracellular SOD activity also increased in the QRY-L group (Figure 6D).

Effect of QRY on Apoptosis in HCE Cells

TUNEL staining showed that 4-HNE induced apoptosis in HCE cells. The results also showed that apoptosis was significantly reduced in the QRY-L and QRY-H groups compared with that in the model group (Figure 6E).

Effect of QRY on Core Targets Expression in HCE Cells Detected by Western Blotting

Activation of the NF-κB and TNF pathways is a crucial manifestation of eye damage induced by oxidative stress.[38,39] Interestingly, both PPI network and KEGG pathway enrichment analyses and molecular docking also indicated that NF-κB and TNF were significant factors in the anti-DED treatment process of QRY. In a follow-up study, we conducted Western blot analysis to evaluate the impact of QRY on key core targets and signaling pathways implicated in oxidative stress. The expression levels of p-P65/P65, TNF-α, IL-1β, and IL-6 were

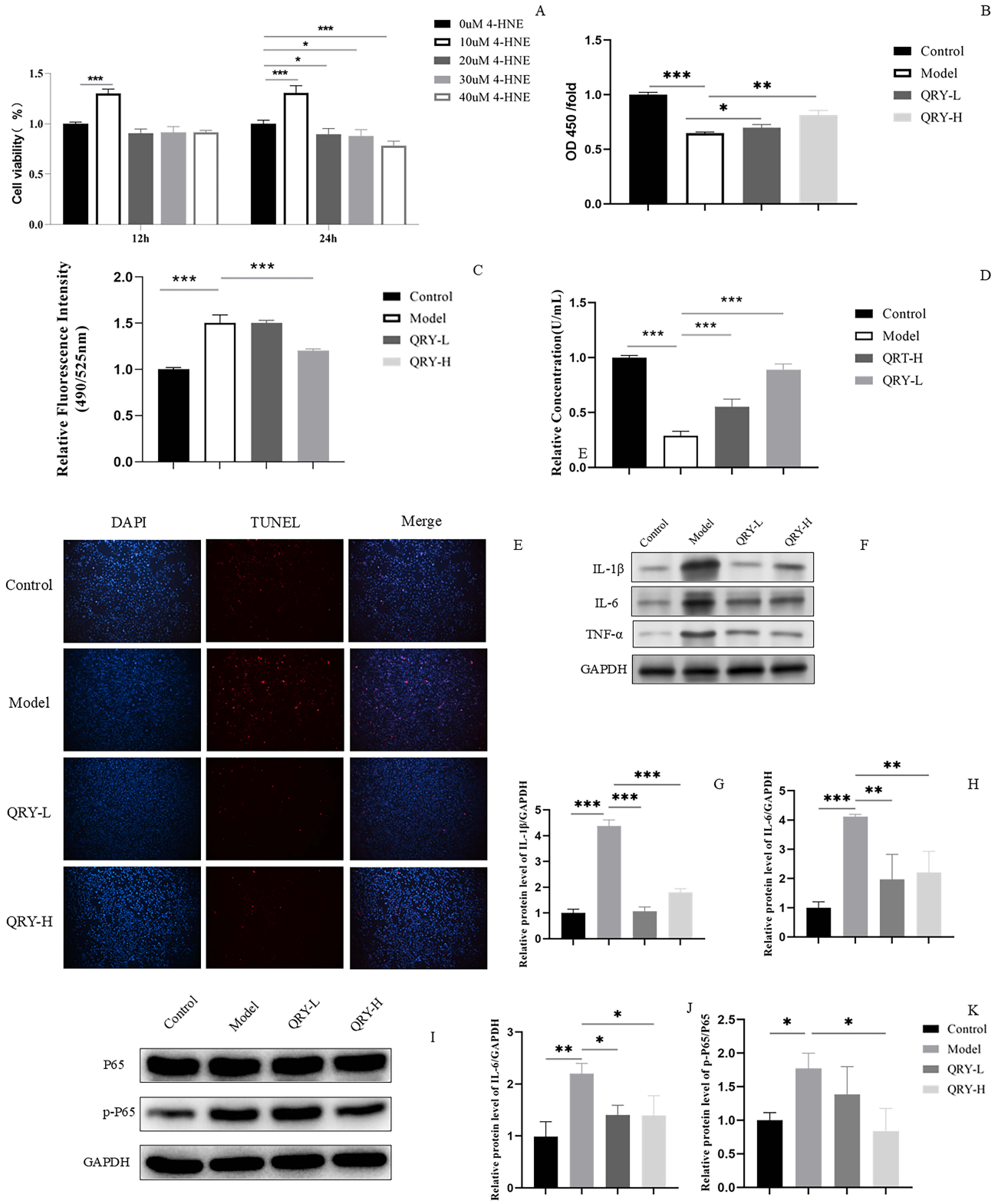

Figure 6 In vitro experiments were performed to verify the anti-oxidative stress effect of QRY. (**A**) CCK8 assay to detect the safety and effective concentration of 4-HNE (n=3-4). (**B**) The effect of QRY on cell viability (n=3-4). (**C**) The effect of QRY on intracellular ROS in HCE cells (n=3). (**D**) ELISA to examine the effect of QRY on intracellular SOD (n=3). (**E**) TUNEL assay showing the effect of QRY on apoptosis. (**F**–**K**) WB verification of the effect of QRY on nucleus targets and pathways (n=3). Data are presented as the $\bar{x} \pm s$. **P* < 0.05, ***P* < 0.01 and ****P* < 0.001vs. Model group.

https://doi.org/10.2147/JIR.S516780

significantly elevated in the model group compared to the controls, reflecting the activation of the NF-κB and TNF pathways. QRY treatment significantly reduced the expression of these markers, particularly in the QRY-H group, confirming its modulatory effects on these markers (Figure 6F–K).

Discussion

ROS play a critical role in ocular physiology. External light penetrates the cornea of the eye into the retina, resulting in oxidative damage, and the antioxidant capacity of the eye decreases progressively with age.[40] Oxidative damage occurs when the natural defense mechanisms of the body are unable to neutralize excess ROS, contributing to various ocular disorders.[41] This damage contributes to various ocular disorders, including DED, glaucoma, age-related macular degeneration (AMD), cataracts, and other corneal disorders.[42–44] Studies have shown that elevated levels of oxidative stress markers, such as 4-HNE and MDA, are strongly correlated with the severity of DED.[34,45] Oxidative stress markers may act as biomarkers of DED, with high ROS levels damaging cellular components, including DNA, proteins, and lipids, leading to inflammation and apoptosis in corneal, conjunctival, and lacrimal gland cells.[9,10,46] Activation of pathways such as NF-κB, TNF, and MAPK by oxidative stress further exacerbates the inflammatory cycle and apoptosis central to DED progression, which is extremely important in the development of DED.[47–49]

Although conventional DED treatments aim to provide symptomatic relief, their efficacy is often short-lived, with limitations including adverse effects and an increased risk of complications such as cataracts and opportunistic infections.[13,14] The anti-oxidative properties of Traditional Chinese Medicine (TCM) offer an alternative therapeutic approach. In this study, Qingxuan Runmu Yin (QRY) demonstrated significant efficacy in mitigating oxidative stress and inflammation in DED, underscoring its potential as a multi-target therapeutic agent.

The current study used a coupled strategy of transcriptomics and network pharmacology to investigate the antioxidant mechanisms of QRY against DED. Our analysis revealed that the main active ingredients of QRY, kaempferol, adenosine, and quercetin, modulate key targets and pathways associated with oxidative stress and inflammation, including IL-1β, IL-6, NF-κB, and TNF. Functional enrichment analyses highlighted QRY's role in response to hypoxia. These findings align with those of previous studies demonstrating the anti-inflammatory and antioxidant properties of individual QRY components such as quercetin, adenosine, and kaempferol. Quercetin, for instance, has been shown to promote corneal repair and inhibit ROS production.[50–52] Similarly, luteolin and kaempferol exhibit protective effects against oxidative and inflammatory damage in ocular tissues.[53,54]

The experimental results further validated QRY's efficacy. QRY alleviated tear secretion deficiency, restored corneal epithelial integrity, and reduced the levels of inflammatory cytokines and ROS in BAC-induced DED mice in vivo. QRY improved cell viability, reduced ROS accumulation, restored SOD activity, and inhibited apoptosis in oxidative stress-induced HCE cells in vitro. These findings strongly suggest that the modulation of oxidative stress is a key mechanism underlying QRY's therapeutic effects in DED.

Network pharmacology is a novel discipline that is useful for analyzing the multi-component and multi-target properties of herbal medicines used to treat diseases. However, the inability to distinguish between inhibitory and activating effects is a disadvantage, which can be compensated for by transcriptomics.[55] Despite these promising results, our study has limitations. The BAC-induced DED model may not fully replicate the complexity of clinical DED, which includes mixed and aqueous-deficient subtypes.[56–58] Additionally, the limited number of RNA-seq replicates may restrict comprehensive identification of target genes. Future studies should explore the effects of QRY in diverse DED models, and expand transcriptomic analyses to include larger sample sizes. Furthermore, the relationship between QRY's multicomponent interactions and its specific molecular mechanisms warrants further investigation.

Conclusion

This study highlights the anti-oxidative stress effects of QRY in DED through modulation of key pathways and targets, providing a scientific foundation for its clinical application. The integration of transcriptomics, network pharmacology, and experimental validation offers a robust framework for elucidating the mechanisms of TCM formulations, paving the way for the development of innovative multi-target therapies for DED and other complex diseases.

Acknowledgments

We thank the online graphic design tool (gdp.renlab.cn) for providing the schematic figures for this study.

Funding

This study was supported by the National Natural Science Foundation of China (81973908). Natural Science Foundation of Heilongjiang Province, China (PL2024H224).

Disclosure

The authors report no conflicts of interest in this work.

References

1. Craig JP, Nichols KK, Akpek EK, et al. TFOS DEWS II definition and classification report. *Ocul Surf*. 2017;15(3):276–283. doi:10.1016/j.jtos.2017.05.008
2. Hakim FE, Farooq AV. Dry eye disease: an update in 2022. *JAMA*. 2022;327(5):478–479. doi:10.1001/jama.2021.19963
3. Bron AJ, de Paiva CS, Chauhan SK, et al. TFOS DEWS II pathophysiology report. *Ocul Surf*. 2017;15(3):438–510. doi:10.1016/j.jtos.2017.05.011
4. Sheppard J, Shen Lee B, Periman LM. Dry eye disease: identification and therapeutic strategies for primary care clinicians and clinical specialists. *Ann Med*. 2023;55(1):241–252. doi:10.1080/07853890.2022.2157477
5. Zhou Y, Murrough J, Yu Y, et al. Association between depression and severity of dry eye symptoms, signs, and inflammatory markers in the DREAM study. *JAMA Ophthalmol*. 2022;140(4):392–399. doi:10.1001/jamaophthalmol.2022.0140
6. Li S, Lu Z, Huang Y, et al. Anti-oxidative and anti-inflammatory micelles: break the dry eye vicious cycle. *Adv Sci (Weinh)*. 2022;9(17):e2200435. doi:10.1002/advs.202200435
7. Saccà SC, Cutolo CA, Ferrari D, Corazza P, Traverso CE. The eye, oxidative damage and polyunsaturated fatty acids. *Nutrients*. 2018;10(6):668. doi:10.3390/nu10060668
8. Dai Y, Zhang J, Xiang J, Li Y, Wu D, Xu J. Calcitriol inhibits ROS-NLRP3-IL-1β signaling axis via activation of Nrf2-antioxidant signaling in hyperosmotic stress stimulated human corneal epithelial cells. *Redox Biol*. 2019;21:101093. doi:10.1016/j.redox.2018.101093
9. Zou H, Wang H, Xu B, Liang L, Shen L, Lin Q. Regenerative cerium oxide nanozymes alleviate oxidative stress for efficient dry eye disease treatment. *Regen Biomater*. 2022;9:rbac070. doi:10.1093/rb/rbac070
10. Dai M, Xu K, Xiao D, et al. In situ forming hydrogel as a tracer and degradable lacrimal plug for dry eye treatment. *Adv Healthc Mater*. 2022;11(19):e2200678. doi:10.1002/adhm.202200678
11. Kwon IS, Kim J, Rhee DK, Kim BO, Pyo S. Pneumolysin induces cellular senescence by increasing ROS production and activation of MAPK/NF-κB signal pathway in glial cells. *Toxicon*. 2017;129:100–112. doi:10.1016/j.toxicon.2017.02.017
12. Chhadva P, Goldhardt R, Galor A. Meibomian gland disease: the role of gland dysfunction in dry eye disease. *Ophthalmology*. 2017;124(11S):S20–S26. doi:10.1016/j.ophtha.2017.05.031
13. Jones L, Downie LE, Korb D, et al. TFOS DEWS II management and therapy report. *Ocul Surf*. 2017;15(3):575–628. doi:10.1016/j.jtos.2017.05.006
14. O'Neil EC, Henderson M, Massaro-Giordano M, Bunya VY. Advances in dry eye disease treatment. *Curr Opin Ophthalmol*. 2019;30(3):166–178. doi:10.1097/ICU.0000000000000569
15. Chan HHL, Lam HI, Choi KY, et al. Delay of cone degeneration in retinitis pigmentosa using a 12-month treatment with Lycium barbarum supplement. *J Ethnopharmacol*. 2019;236:336–344. doi:10.1016/j.jep.2019.03.023
16. Feng Z, Fu L, Wang J, et al. Efficacy of tripterygium glycosides (TG) in rheumatoid arthritis as a disease-modifying anti-rheumatic drug (DMARD) in combination with conventional DMARDs: a systematic review and meta-analysis of randomized controlled trials. *Pharmacol Res*. 2022;184:106405. doi:10.1016/j.phrs.2022.106405
17. Wang JD, An BP, Liu Y, et al. Clinical trial of qingxuan runmu yin granules in the treatment of dry eye patients with diabetes. *Chin. J. Clin. Pharmacol*. 2023;39(22):3257–3261. doi:10.13699/j.cnki.1001-6821.2023.22.014
18. Wang J, Liu Y, Zong B, et al. Qingxuan Runmu Yin alleviates dry eye disease via inhibition of the HMOX1/HIF-1 pathway affecting ferroptosis. *Front Pharmacol*. 2024:15. doi:10.3389/fphar.2024.1391946
19. Yu J, Wang S, Yang J, et al. Exploring the mechanisms of action of Zengye decoction (ZYD) against Sjogren's syndrome (SS) using network pharmacology and animal experiment. *Pharm Biol*. 2023;61(1):1286–1297. doi:10.1080/13880209.2023.2248188
20. Ling J, Chan CL, Ho CY, et al. The extracts of dendrobium alleviate dry eye disease in rat model by regulating aquaporin expression and MAPKs/NF-κB signalling. *Int J Mol Sci*. 2022;23(19):11195. doi:10.3390/ijms231911195
21. Wu JY, Chen YJ, Bai L, et al. Chrysoeriol ameliorates TPA-induced acute skin inflammation in mice and inhibits NF-κB and STAT3 pathways. *Phytomedicine*. 2020;68:153173. doi:10.1016/j.phymed.2020.153173
22. Kim MH, Kwon SY, Woo SY, Seo WD, Kim DY. Antioxidative effects of chrysoeriol via activation of the Nrf2 signaling pathway and modulation of mitochondrial function. *Molecules*. 2021;26(2):313. doi:10.3390/molecules26020313
23. Ma XY, Wen XX, Yang XJ, et al. Ophiopogonin D improves osteointegration of titanium alloy implants under diabetic conditions by inhibition of ROS overproduction via Wnt/β-catenin signaling pathway. *Biochimie*. 2018;152:31–42. doi:10.1016/j.biochi.2018.04.022
24. Huang Z, Sheng Y, Chen M, Hao Z, Hu F, Ji L. Liquiritigenin and liquiritin alleviated MCT-induced HSOS by activating Nrf2 antioxidative defense system. *Toxicol Appl Pharmacol*. 2018;355:18–27. doi:10.1016/j.taap.2018.06.014
25. Krstić L, Jarho P, Ruponen M, Urtti A, González-García MJ, Diebold Y. Improved ocular delivery of quercetin and resveratrol: a comparative study between binary and ternary cyclodextrin complexes. *Int J Pharm*. 2022;624:122028. doi:10.1016/j.ijpharm.2022.122028

26. Okonkwo A, Rimmer V, Walkden A, et al. Next-generation sequencing of the ocular surface microbiome: in health, contact lens wear, diabetes, trachoma, and dry eye. *Eye Contact Lens*. 2020;46(4):254–261. doi:10.1097/ICL.0000000000000697
27. Hu X, Qi C, Feng F, et al. Combining network pharmacology, RNA-seq, and metabolomics strategies to reveal the mechanism of cimicifugae rhizoma - smilax glabra Roxb herb pair for the treatment of psoriasis. *Phytomedicine*. 2022;105:154384. doi:10.1016/j.phymed.2022.154384
28. Wang B, Peng L, Ouyang H, et al. Induction of DDIT4 impairs autophagy through oxidative stress in dry eye. *Invest Ophthalmol Vis Sci*. 2019;60 (8):2836–2847. doi:10.1167/iovs.19-27072
29. Yang FM, Fan D, Yang XQ, et al. The artemisinin analog SM934 alleviates dry eye disease in rodent models by regulating TLR4/NF-κB/NLRP3 signaling. *Acta Pharmacol Sin*. 2021;42(4):593–603. doi:10.1038/s41401-020-0484-5
30. Kopylova E, Noé L, Touzet H. SortMeRNA: fast and accurate filtering of ribosomal RNAs in metatranscriptomic data. *Bioinformatics*. 2012;28 (24):3211–3217. doi:10.1093/bioinformatics/bts611
31. Bolger AM, Lohse M, Usadel B. Trimmomatic: a flexible trimmer for illumina sequence data. *Bioinformatics*. 2014;30(15):2114–2120. doi:10.1093/bioinformatics/btu170
32. Kim D, Langmead B, Salzberg SL. HISAT: a fast spliced aligner with low memory requirements. *Nat Methods*. 2015;12(4):357–360. doi:10.1038/nmeth.3317
33. Chen JY, Yang YJ, Meng XY, et al. Oxysophoridine inhibits oxidative stress and inflammation in hepatic fibrosis via regulating Nrf2 and NF-κB pathways. *Phytomedicine*. 2024;132:155585. doi:10.1016/j.phymed.2024.155585
34. Choi W, Lian C, Ying L, et al. Expression of lipid peroxidation markers in the tear film and ocular surface of patients with non-sjogren syndrome: potential biomarkers for dry eye disease. *Curr Eye Res*. 2016;41(9):1143–1149. doi:10.3109/02713683.2015.1098707
35. Liu H, Gambino F, Algenio CS, et al. Inflammation and oxidative stress induced by lipid peroxidation metabolite 4-hydroxynonenal in human corneal epithelial cells. *Graefes Arch Clin Exp Ophthalmol*. 2020;258(8):1717–1725. doi:10.1007/s00417-020-04647-2
36. Zheng X, Cui H, Yin Y, et al. SERPINA3K ameliorates the corneal oxidative injury induced by 4-hydroxynonenal. *Invest Ophthalmol Vis Sci*. 2017;58(7):2874–2883. doi:10.1167/iovs.17-21544
37. Zhang Y, Sano M, Shinmura K, et al. 4-Hydroxy-2-nonenal protects against cardiac ischemia–reperfusion injury *via* the Nrf2-dependent pathway. *J Mol Cellular Cardiol*. 2010;49(4):576–586. doi:10.1016/j.yjmcc.2010.05.011
38. Vernazza S, Tirendi S, Bassi AM, Traverso CE, Saccà SC. Neuroinflammation in primary open-angle glaucoma. *J Clin Med*. 2020;9(10). doi:10.3390/jcm9103172
39. Areesanan A, Nicolay S, Keller M, Zimmermann-Klemd AM, Potterat O, Gründemann C. Potential benefits of Malva sylvestris in dry-eye disease pathology in vitro based on antioxidant, wound-healing and anti-inflammatory properties. *Biomed Pharmacother*. 2023;168:115782. doi:10.1016/j.biopha.2023.115782
40. Salceda R. Light pollution and oxidative stress: effects on retina and human health. *Antioxidants*. 2024;13(3):362. doi:10.3390/antiox13030362
41. Ung L, Pattamatta U, Carnt N, Wilkinson-Berka JL, Liew G, White AJR. Oxidative stress and reactive oxygen species: a review of their role in ocular disease. *Clin Sci*. 2017;131(24):2865–2883. doi:10.1042/CS20171246
42. Beatty S, Koh H, Phil M, Henson D, Boulton M. The role of oxidative stress in the pathogenesis of age-related macular degeneration. *Surv Ophthalmol*. 2000;45(2):115–134. doi:10.1016/s0039-6257(00)00140-5
43. Li L, Duker JS, Yoshida Y, et al. Oxidative stress and antioxidant status in older adults with early cataract. *Eye*. 2009;23(6):1464–1468. doi:10.1038/eye.2008.281
44. Zhao J, Wang S, Zhong W, Yang B, Sun L, Zheng Y. Oxidative stress in the trabecular meshwork (Review). *Int J Mol Med*. 2016;38(4):995–1002. doi:10.3892/ijmm.2016.2714
45. Navel V, Sapin V, Henrioux F, et al. Oxidative and antioxidative stress markers in dry eye disease: a systematic review and meta-analysis. *Acta Ophthalmol*. 2022;100(1):45–57. doi:10.1111/aos.14892
46. Kruk J, Kubasik-Kladna K, Aboul-Enein HY. The role oxidative stress in the pathogenesis of eye diseases: current status and a dual role of physical activity. *Mini Rev Med Chem*. 2015;16(3):241–257. doi:10.2174/1389557516666151120114605
47. Baeuerle PA, Baltimore D. NF-kappa B: ten years after. *Cell*. 1996;87(1):13–20. doi:10.1016/s0092-8674(00)81318-5
48. Krishnamoorthy RR, Crawford MJ, Chaturvedi MM, et al. Photo-oxidative stress down-modulates the activity of nuclear factor-kappaB via involvement of caspase-1, leading to apoptosis of photoreceptor cells. *J Biol Chem*. 1999;274(6):3734–3743. doi:10.1074/jbc.274.6.3734
49. Pflugfelder SC, Stern ME. The cornea in keratoconjunctivitis sicca. *Experimental Eye Research*. 2020;201:108295. doi:10.1016/j.exer.2020.108295
50. Abengózar-Vela A, Schaumburg CS, Stern ME, Calonge M, Enríquez-de-Salamanca A, González-García MJ. Topical quercetin and resveratrol protect the ocular surface in experimental dry eye disease. *Ocul Immunol Inflamm*. 2019;27(6):1023–1032. doi:10.1080/09273948.2018.1497664
51. Inaba T, Ohnishi-Kameyama M, Liu Y, et al. Quercetin improves lacrimal gland function through its anti-oxidant actions: evidence from animal studies, and a pilot study in healthy human volunteers. *Front Nutr*. 2022;9:974530. doi:10.3389/fnut.2022.974530
52. Huang L, Kim MY, Cho JY. Immunopharmacological activities of luteolin in chronic diseases. *Int J Mol Sci*. 2023;24(3):2136. doi:10.3390/ijms24032136
53. Al Sabaani N. Kaempferol protects against hydrogen peroxide-induced retinal pigment epithelium cell inflammation and apoptosis by activation of SIRT1 and inhibition of PARP1. *J Ocul Pharmacol Ther*. 2020;36(7):563–577. doi:10.1089/jop.2019.0151
54. Chuang YL, Fang HW, Ajitsaria A, et al. Development of kaempferol-loaded gelatin nanoparticles for the treatment of corneal neovascularization in mice. *Pharmaceutics*. 2019;11(12):635. doi:10.3390/pharmaceutics11120635
55. Zhu H, Wang S, Shan C, et al. Mechanism of protective effect of xuan-bai-cheng-qi decoction on LPS-induced acute lung injury based on an integrated network pharmacology and RNA-sequencing approach. *Respir Res*. 2021;22(1):188. doi:10.1186/s12931-021-01781-1
56. Zhu J, Inomata T, Shih KC, et al. Application of animal models in interpreting dry eye disease. *Front Med*. 2022;9:830592. doi:10.3389/fmed.2022.830592
57. Kessal K, Daull P, Cimbolini N, et al. Comparison of two experimental mouse dry eye models through inflammatory gene set enrichment analysis based on a multiplexed transcriptomic approach. *Int J Mol Sci*. 2021;22(19):10770. doi:10.3390/ijms221910770
58. Chaudhari P, Satarker S, Thomas R, et al. Rodent models for dry eye syndrome: standardization using benzalkonium chloride and scopolamine hydrobromide. *Life Sciences*. 2023;317:121463. doi:10.1016/j.lfs.2023.121463